STRONG MOTION RECORDS FROM THE KOBE, JAPAN EARTHQUAKE OF JAN. 17, 1995, AND IMPLICATIONS FOR SEISMIC HAZARDS IN CALIFORNIA

Paul Somerville

Woodward-Clyde Federal Services
Pasadena, California

ABSTRACT

The strong ground motion characteristics of the Kobe earthquake are very similar to those of California earthquakes. This raises the question of whether losses as large as the $200 billion which occurred in Kobe could occur in an urban earthquake in California.

INTRODUCTION

The January 17, 1995 Hyogo Ken Nanbu Earthquake is the most damaging earthquake to have struck Japan since the great Kanto earthquake destroyed large areas of Tokyo and Yokohama and killed approximately 150,000 people (mostly by fire) in 1923. As of February 17, the toll from the Kobe earthquake had reached 5,368 dead and 26,815 injured. It is estimated that 144,032 buildings were destroyed by ground shaking and 7,456 buildings were destroyed by fire. The number of homeless people requiring shelter was approximately 300,000, which is 20% of the population of Kobe. Current estimates of losses in this city of 1.5 million people are about 20 trillion yen (200 billion dollars). This includes approximately $100 billion estimated by the Hyogo Prefectural Government to restore basic functions, approximately $50 billion in losses of private property, and approximately $50 billion in losses due to economic dislocation and business interruption. This paper describes ground motion data relevant to the question of whether these very large losses, which are an order of magnitude larger than those from the January 17, 1994 Northridge, California earthquake, could occur in an earthquake in an urban region of California.

SOURCE CHARACTERISTICS OF THE KOBE EARTHQUAKE

The tectonic setting and source characteristics of the Kobe earthquake have been described by Kanamori (1995) and Somerville (1995a,b). The time sequence and orientation of faulting during the Kobe earthquake has been inferred from the analysis of strong motion data by Pitarka et al. (1995) and teleseismic data by Kikuchi (1995). The fit of recorded and synthetic velocity waveforms in the Pitarka et al. (1995) model is shown in Figure 1. Southwest of the epicenter, away from Kobe, the earthquake produced 11 km of surface rupture with an average horizontal displacement of 1 to 1.5 meters on the Nojima fault, which runs along the northwest shore of Awaji Island. The strike-slip motion was accompanied by a component of thrust motion, producing a fault scarp dipping down to the southeast, with the northwest side down. This dip is consistent with the offset of the surface rupture by a few km to the northwest from the epicenter, and with the focal mechanism of the first event as inferred by Kikuchi (1995) and Pitarka et al. (1995). The dip direction is reversed on the part of the rupture that extends

northeast from the epicenter toward Kobe. A releveling survey after the earthquake found a decrease in elevation of 26 cm between Tarumi and Suma Wards in western Kobe, inferred to mark the location of subsurface faulting. This down to the southeast faulting on a fault plane dipping down to the northwest is seen in the focal mechanisms of later subevents in the rupture model of Pitarka et al. (1995, Figure 1). Both the Kikuchi and Pitarka rupture models indicate that the propagation of the rupture toward Kobe involved several subevents distributed along the fault at depths of 6 to 8 km. The Pitarka model has uniform strike but variations in dip and rake among three subevents (Figure 1), while the Kikuchi model has variations in strike as well as variations in rake of two subevents.

STRONG MOTION CHARACTERISTICS OF THE KOBE EARTHQUAKE

Strong ground motions were recorded by numerous organizations, including the Committee on Earthquake Observation and Research in the Kansai Area, Japan Rail, Osaka Gas, JMA, Hankyu Railroads, Japan Highways, Building Research Institute, and Port and Harbor Research Institute. The largest recorded peak accelerations were about 0.8g (Figure 2), and were recorded on alluvial sites. The vertical peak accelerations were generally about two-thirds as large as the horizontal at near-fault sites, and much lower at more distant alluvial sites.

The rupture of this strike-slip earthquake directly into downtown Kobe caused near-fault rupture directivity effects which appear to have contributed to the high level of damage. The recorded peak velocities were as large as 175 cm/sec at Takatori in western Kobe, and the largest values occurred in the densely populated urban region, as shown in Figure 3a. Currently, buildings over 60 meters in height in Japan are designed to withstand peak velocities of 50 cm/sec without collapse. The near-fault ground velocity time histories have large, brief pulses of ground motion (Figure 4) that are indicative of rupture directivity effects and are potentially damaging to multi-story buildings and other long-period structures such as bridges. The horizontal motions in the fault normal direction are about twice as large as those in the fault parallel direction, as seen in the time histories in Figure 4 and the response spectra in Figure 5. This feature, which is caused by rupture directivity effects, has been widely observed in near fault strong motion data in California (Somerville and Graves, 1993) and quantified as a modification to empirical attenuation relations by Somerville and Graves (1995).

Severe damage to buildings due to the Kobe earthquake was observed along a strip of land about 30 km long and 1 km wide, and offset about 1 km southeast of the fault. Figure 6 shows the severely damaged area, active faults, and aftershock distribution (Kohketsu, 1995). The hachured zone indicates the area where the rate of collapsed wood-frame buildings is more than 30%; this rate exceeded 70% in the central part of this area. There are few aftershocks and active faults in the severely damaged area, suggesting that the location of the severely damaged area is not explained by its proximity to the fault rupture.

In order to investigate whether these large variations in site response in the Kobe area were attributable to site effects, investigators from Ohsaki Research Institute recorded aftershocks at several sites on alluvium in the heavily damaged area as well as at rock sites on the foot of Rokko mountain in Kobe (Kawase et al, 1995). The locations of their stations are shown in Figure 7a and their study area is shown as an inset in Figure 6. They found that, for six

aftershocks, horizontal peak accelerations recorded at three sites located on a thin layer of soft alluvium (about 10 to 15 meters thick) were about 3 to 5 times larger than those at a reference site on rock, and the Fourier spectral amplitudes for frequencies between 2 and 3 Hz were as much as 20 times higher, as shown in Figure 7b.

IMPLICATIONS FOR SEISMIC HAZARDS IN CALIFORNIA

There are many parallels between the seismic hazard environment in Kobe and those that are present in urban regions in California. Figure 8 shows active faults and the surficial geology of the San Francisco Bay region. The many similarities between Kobe and the East San Francisco Bay region are illustrated by comparison of Figure 8 with Figure 6, and the comparison of geological cross sections through Kobe and Oakland shown in Figure 9. These similarities include the location of strike-slip faults along the base of the mountains; the increasing thickness of alluvial deposits from the mountains to the bay shore; and the highly urbanized areas located on soft sediments between the mountains and the shore.

The recorded peak accelerations and velocities from the Kobe earthquake are generally comparable to those predicted for a strike-slip earthquake using empirical attenuation relations for soil based mainly on California data (Abrahamson and Silva, 1995; Campbell, 1990), as shown in Figure 10. The much larger level of damage that occurred in the Kobe earthquake compared with that of recent earthquakes in California may be partly attributable to the fact that the dense urban region of Kobe was subject to strong rupture directivity effects. As shown in Figure 3a, the largest peak velocities recorded from the Kobe earthquake were in the dense urban region. Equally large peak velocities were recorded during the 1994 Northridge earthquake, as shown in Figure 3b. However, the dense urban regions of the southern San Fernando Valley and the northwest Los Angeles basin were not subject to rupture directivity effects. Almost all of the faulting occurred at depths greater than 10 km, and the great majority of the multi-story buildings in the San Fernando Valley were at least 15 km from the closest part of the fault. Rupture directivity effects were experienced only in the northern San Fernando Valley and Santa Susana Mountains, which are located away from the dense urban region.

There are many densely populated urban regions in California that are located very close to major strike-slip faults. However, California has not experienced a strike-slip earthquake that ruptured directly into a heavily populated urban region since the 1933 Long Beach earthquake, and has no experience of a strike-slip earthquake rupturing into the downtown region of a major city. We do not have data from California on the performance of structures exposed to rupture directivity effects from a strike-slip earthquake that ruptured directly into an urban region, as occurred in Kobe. However, the apparent similarity in earthquake source and strong ground motion characteristics between the Kobe earthquake and California earthquakes indicates that the performance of soils and structures in the Kobe earthquake may be very useful for predicting damage effects from an urban strike-slip earthquake in California.

Given the widespread damage that occurred in Kobe, and the apparent parallels between the strong ground motions experienced there and those that we expect in California, it is important to make loss estimates for urban strike-slip earthquakes in California based on the performance data from Kobe, and to assess whether they may greatly exceed those of the 1994

Northridge earthquake. If it is concluded that losses of Kobe proportions could occur in an urban strike-slip earthquake in California, this could have important implications for code provisions and other policy decisions concerning the reduction of earthquake damage in the United States.

REFERENCES

Kanamori, H. (1995). The Kobe (Hyogo-ken Nanbu), Japan, earthquake of January 16, 1995. Seismological Research Letters 66, 6-10.

Kawase, H., T. Satoh and S. Matsushima (1995). Aftershock measurements and a preliminary analysis of aftershock records in Higashi-Nada Ward in Kobe after the 1995 Hyogo-Ken-Nanbu earthquake, ORI Report 94-04.

Kohketsu, K. (1995). Are predominant period contents of strong-motions the major cause of severe damage by the Kobe earthquake?, Monthly Journal of Science, Kagaku Asahi, No. 652, 11-14.

Kikuchi, M., Teleseismic analysis of the Southern Hyogo (Kobe), Japan, earthquake of January 17, 1995, Yokohama City University Seismological Note #38, 1995.

Pitarka, A., K. Irikura and T. Kagawa (1995). Source complexity of the January 17, 1995 Hyogo-ken-nanbu earthquake from nearfield strong motion modeling: preliminary results. Submitted to Journal of Natural Disaster Science.

Research Group for Active Faults in Japan (1980). Maps of Active Faults in Japan with an Explanatory Text, University of Tokyo Press, Hongo, Bunkyo-ku, Tokyo 113, Japan.

Rogers, J.D. and S.H. Figuers (1991). Engineering geologic site characterization of the greater Oakland-Alameda area. Alameda and San Francisco Counties, California. Final Report to the National Science Foundation, Grant No. BCS-9003785.

Somerville, P.G. (1995a). Kobe Earthquake: an Urban Disaster. EOS 76, 49-51.

Somerville, P.G. (1995b). Kobe Earthquake : Geoscience and Strong Motion Apects, in EERI Reconnaissance Report, Chapter 1, pp. 1-10.

Somerville, P.G. and R.W. Graves (1995). Ground motion potential of the Los Angeles Region. *Proceedings of the 1995 Annual Meeting of the Los Angeles Tall Buildings Structural Design Council*, May 5.

Somerville, P.G. and R.W. Graves (1993). Conditions that give rise to unusually large long period ground motions, *The structural design of tall buildings* 2, 211-232.

Takeo, M. (1995). Rupture model of the Kobe earthquake inferred from strong motion data. Poster presented at the Annual Meeting of the Seismological Society of Japan, March 27-30, Tokyo.

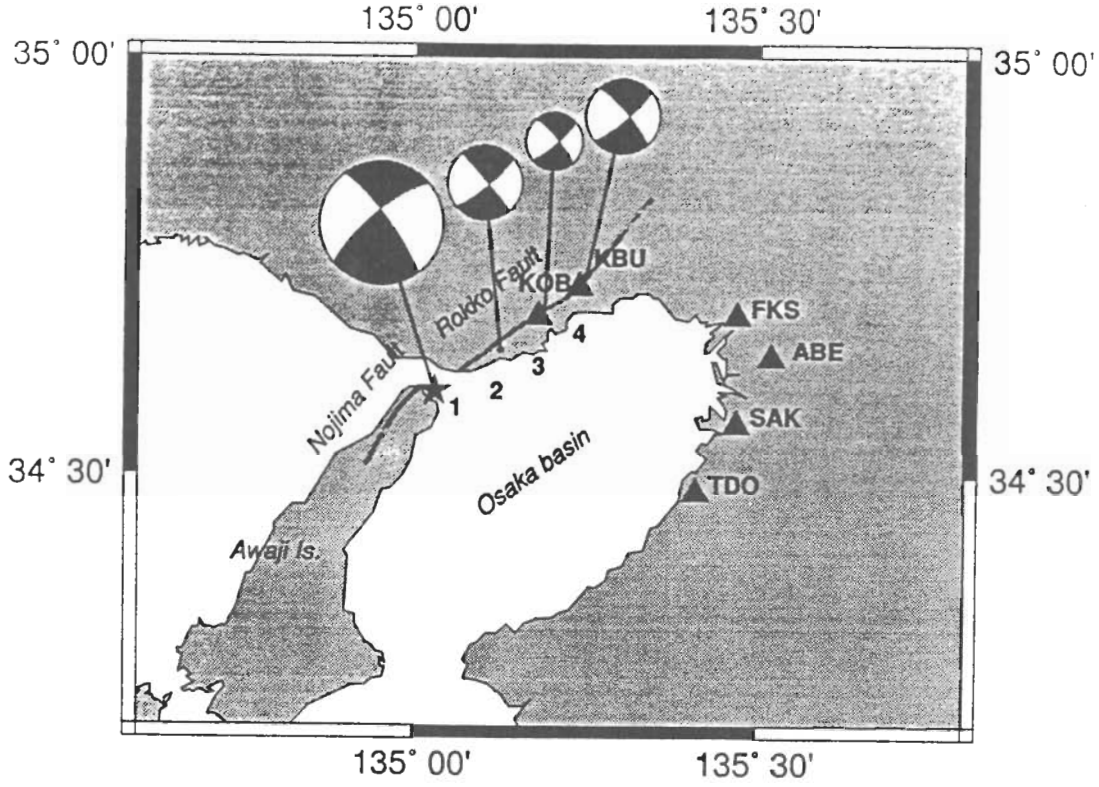

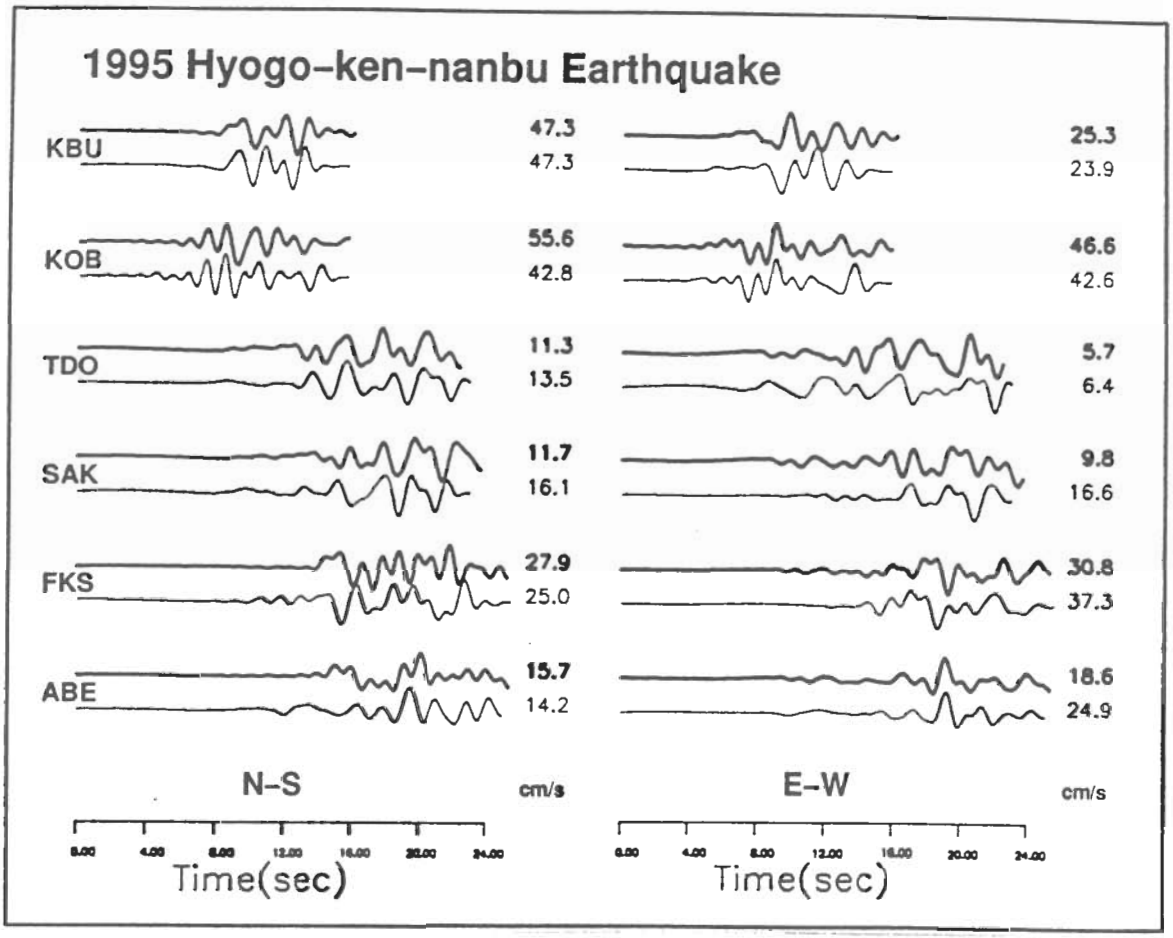

Figure 1. Focal mechanism and source process of the Kobe earthquake. The earthquake consisted of four subevents, whose locations and focal mechanisms are shown at the top. Recorded and synthetic waveforms are compared at the bottom. Source: Pitarka et al., 1995.

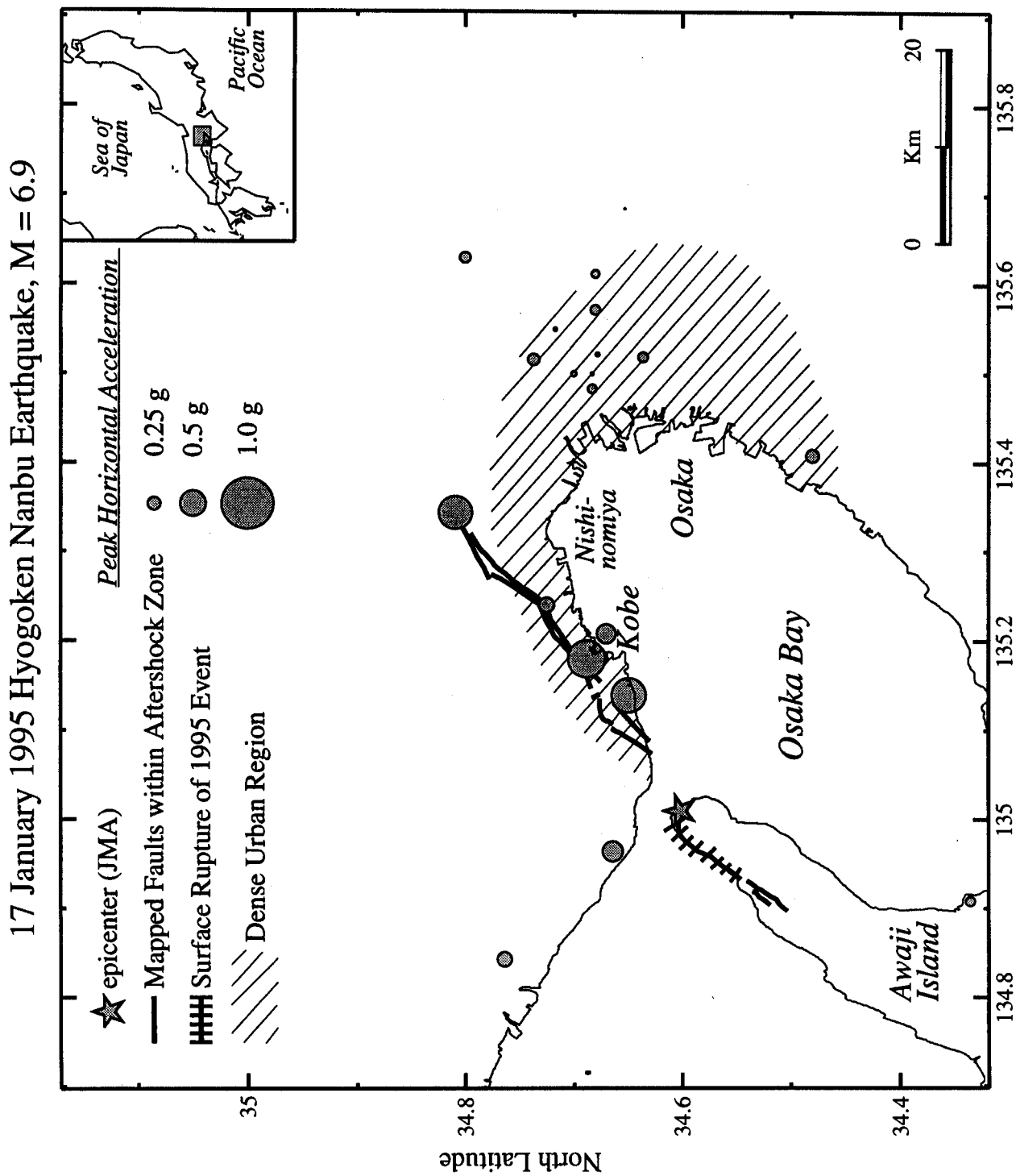

Figure 2. Location of the mainshock epicenter, mapped active faults within the aftershock zone (including surface rupture of the Nojima fault on Awaji Island), the dense urban region, and average horizontal peak accelerations recorded from the 1995 Kobe earthquake.

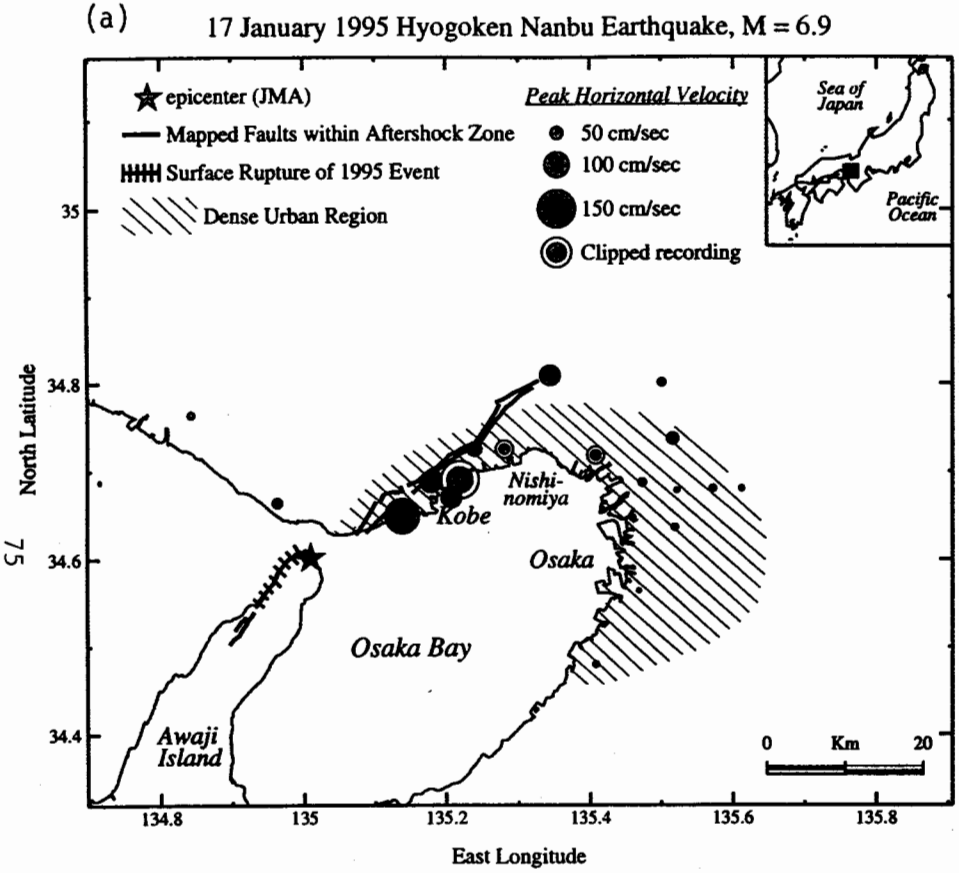

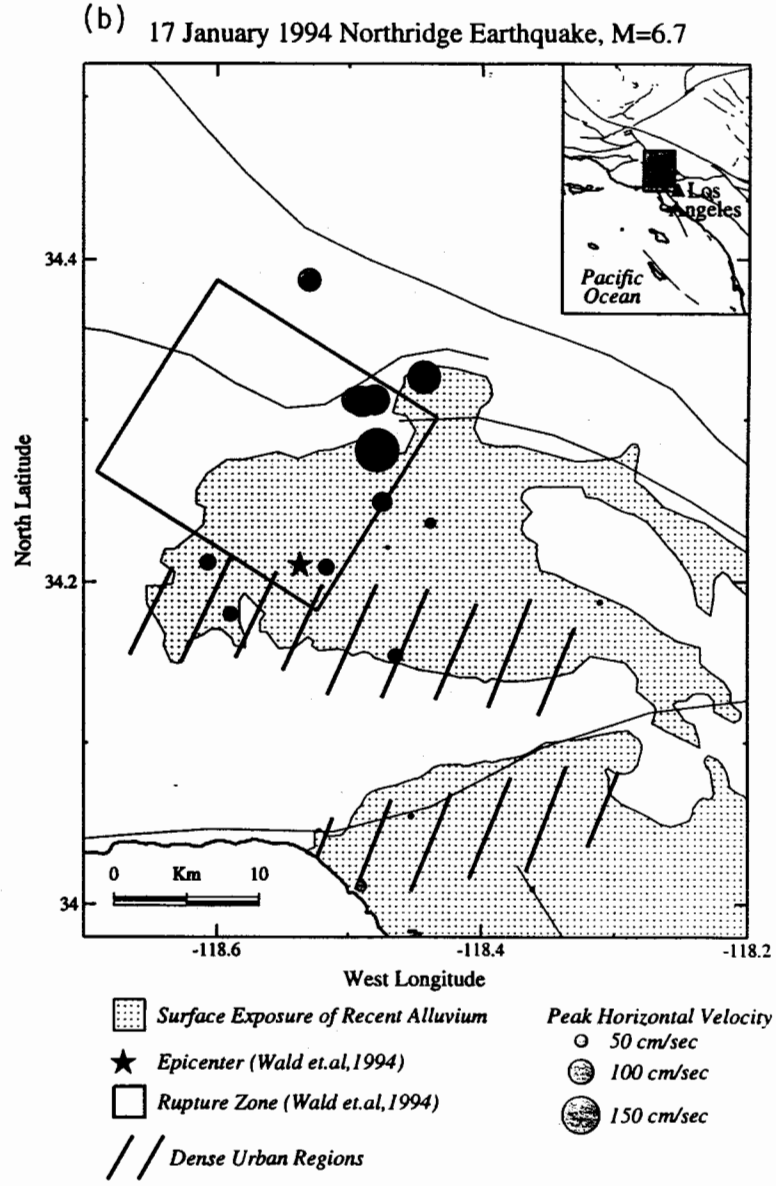

Figure 3 (a) Location of the mainshock epicenter, mapped active faults within the aftershock zone (including surface rupture of the Nojima fault on Awaji Island), the dense urban region, and average horizontal peak velocities recorded from the 1995 Kobe earthquake. (b) Location of the mainshock epicenter, surface projection of the fault rupture model of Wald and Heaton (1994), dense urban regions, and average horizontal peak ground velocities recorded from the 1994 Northridge earthquake.

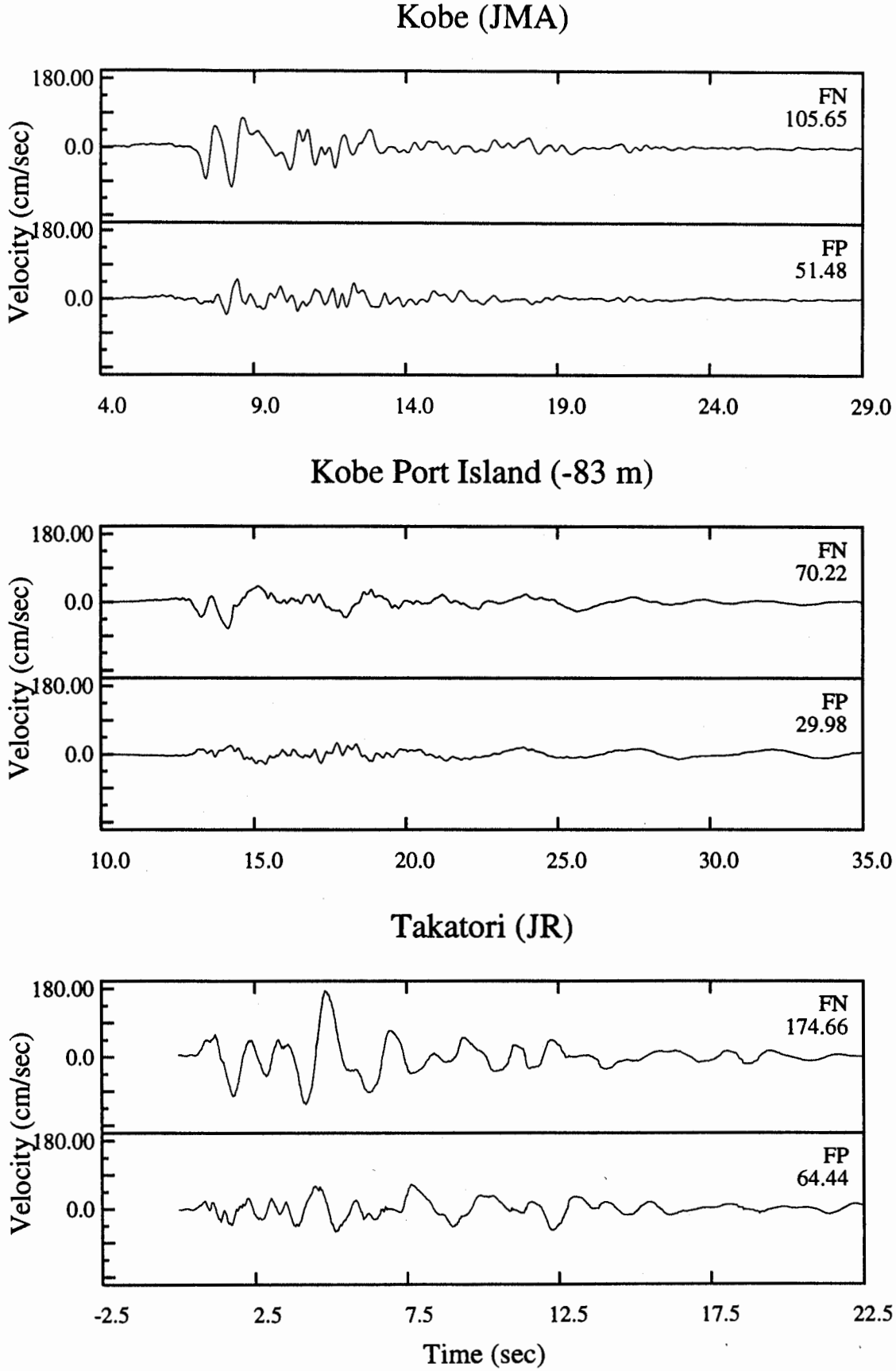

Figure 4. Recorded velocity time histories at Kobe JMA, Port Island -83 meters, and Takatori rotated into fault-normal and fault-parallel components.

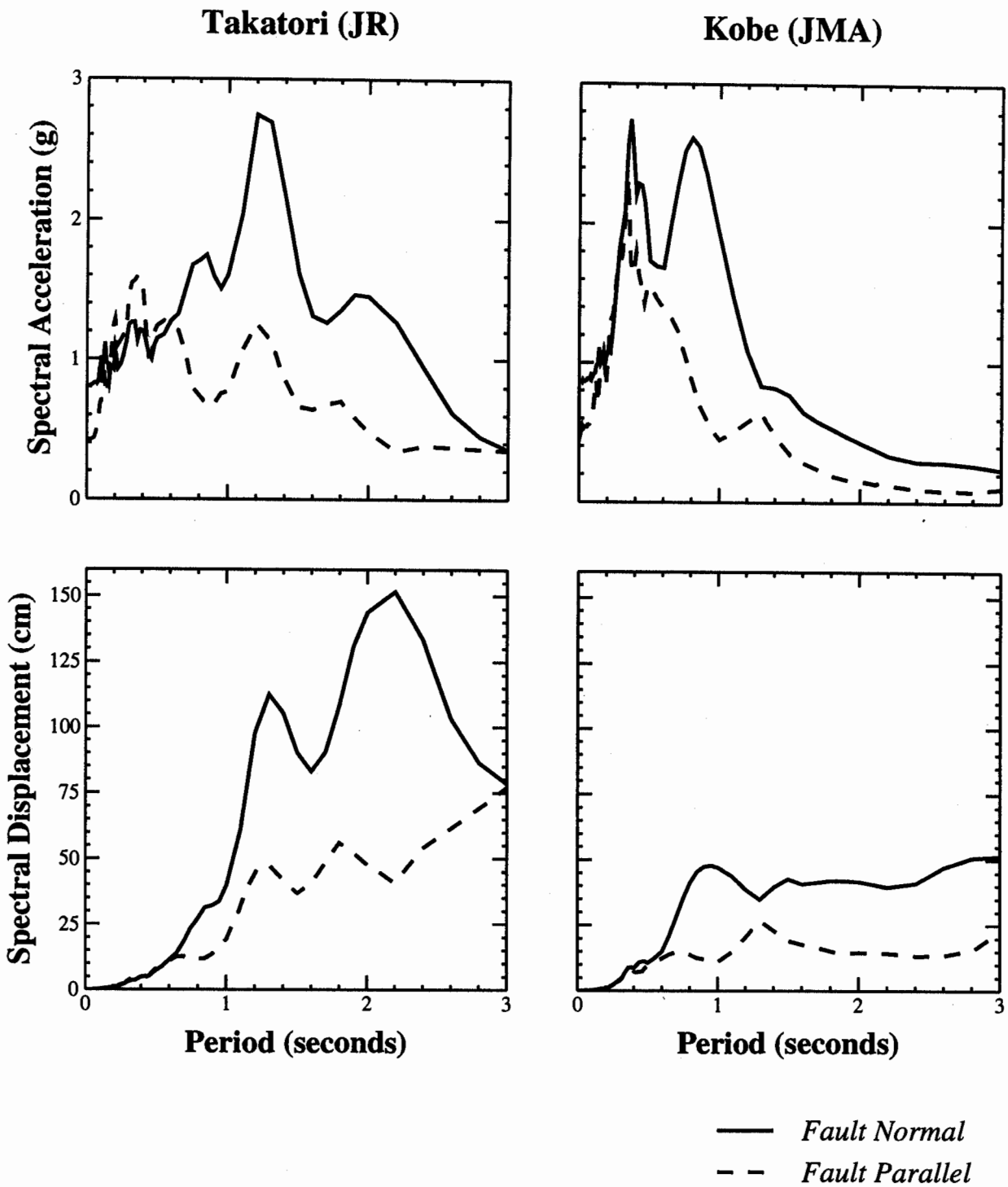

Figure 5. Response spectral acceleration (top) and displacement (bottom) of the fault-normal and fault-parallel components of the Kobe earthquake recorded at Kobe JMA and Takatori.

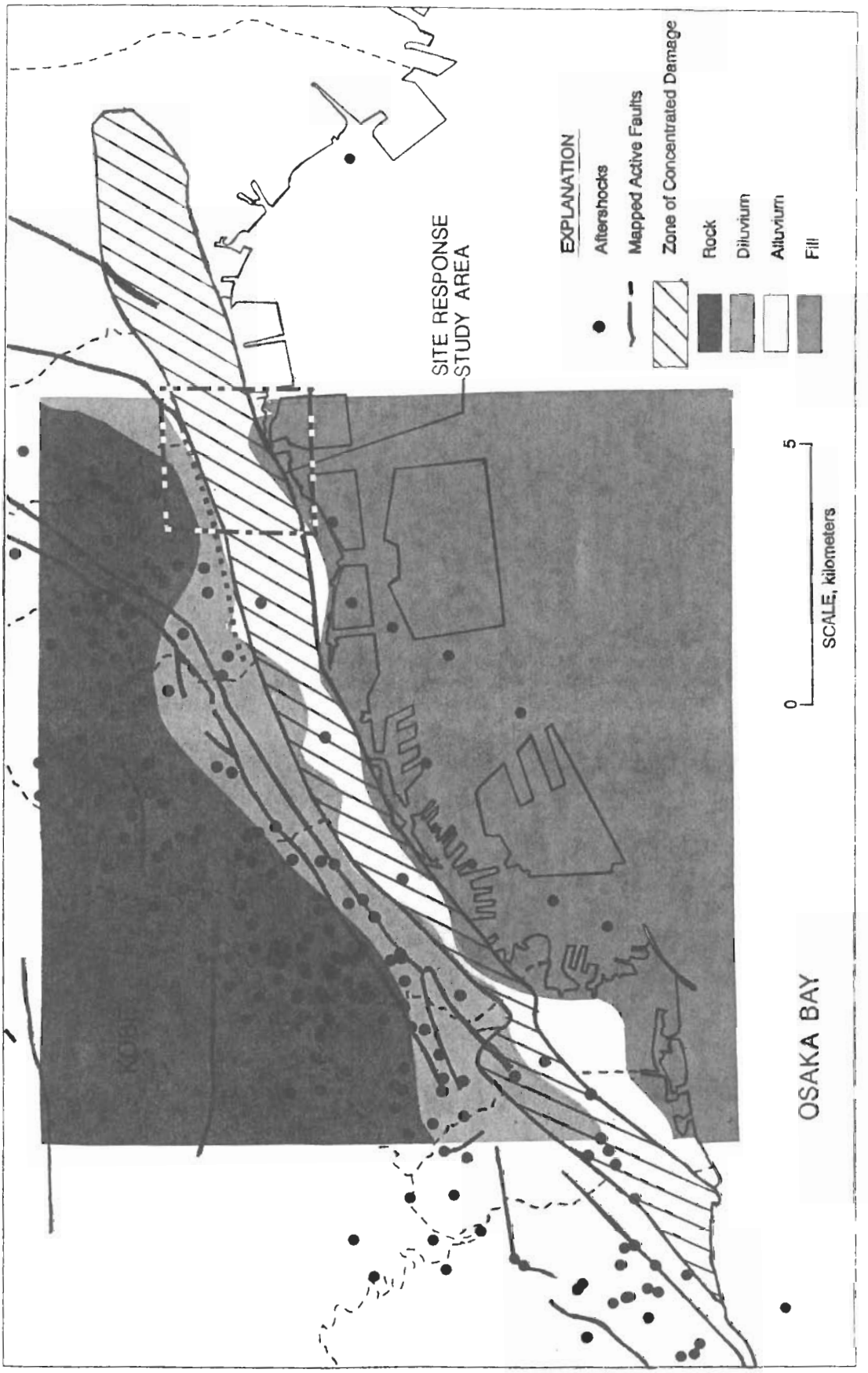

Figure 6. Location of zone of intense destruction in the Kobe area, and its relationship to the location of active faults, the aftershock distribution, and geological site conditions. Modified from Kohketsu, 1995.

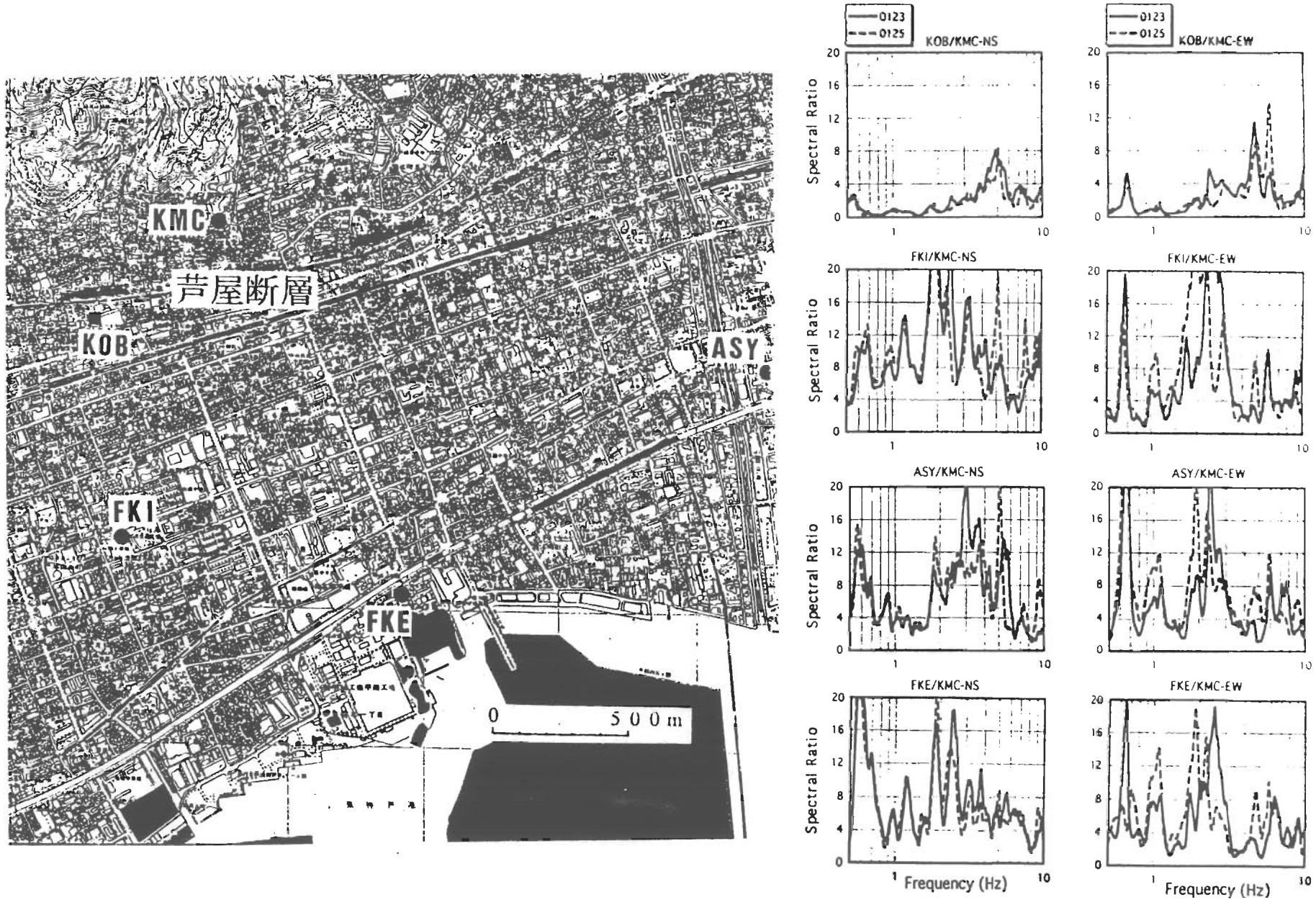

Figure 7. Left: Locations of aftershock recording sites used in the site response study conducted by Kawase et al. (1995). The location of the study area is shown in Figure 6. Right: Fourier spectral ratios for two aftershocks and referenced to rock site KMC for diluvial site KOB, alluvial sites FKI and ASY, and fill site FKE. Source: Kawase et al. (1995).

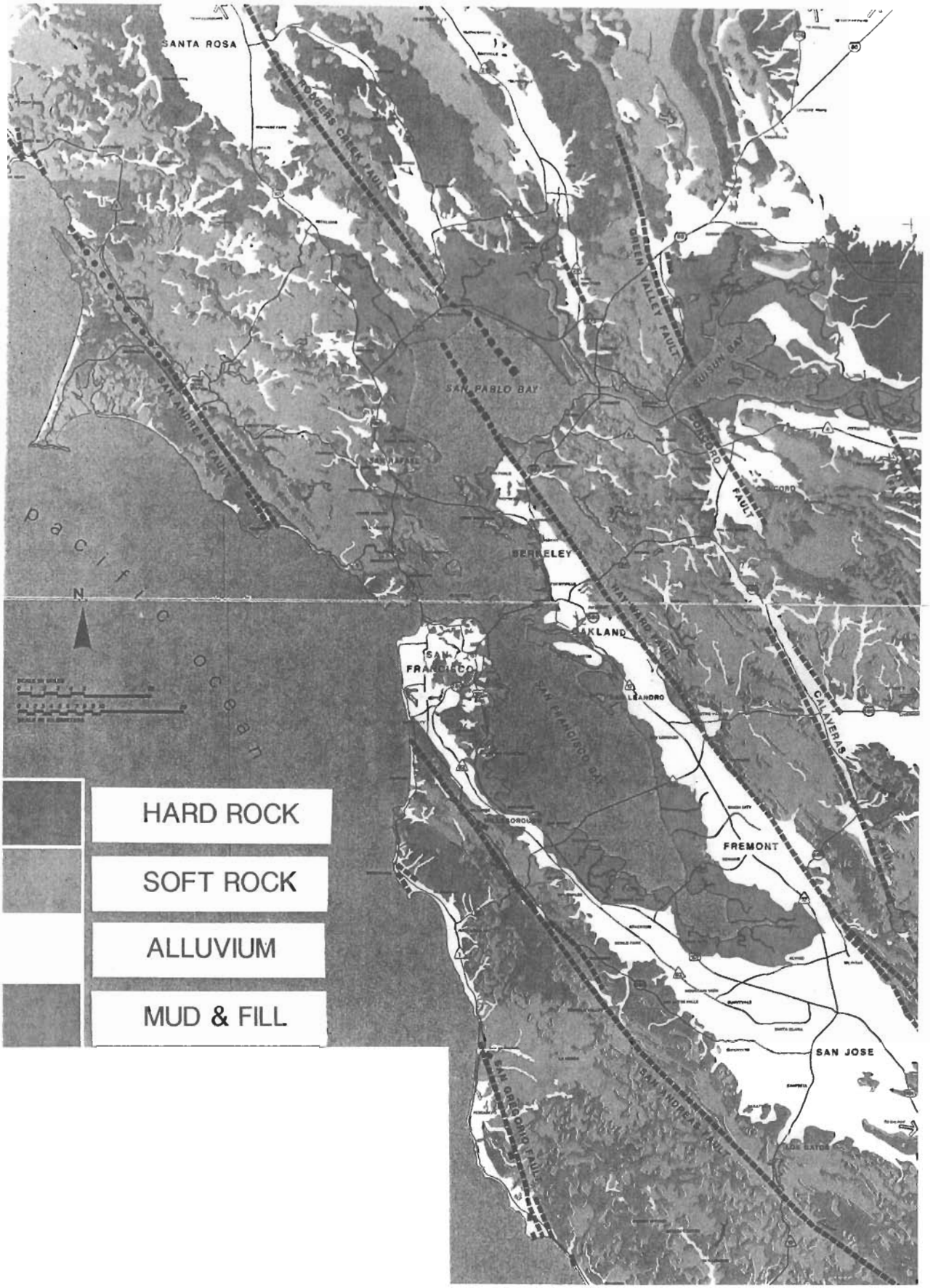

Figure 8. Map of the San Francisco Bay area showing the location of the Hayward fault and the distribution of surface geology. Source: United States Geological Survey.

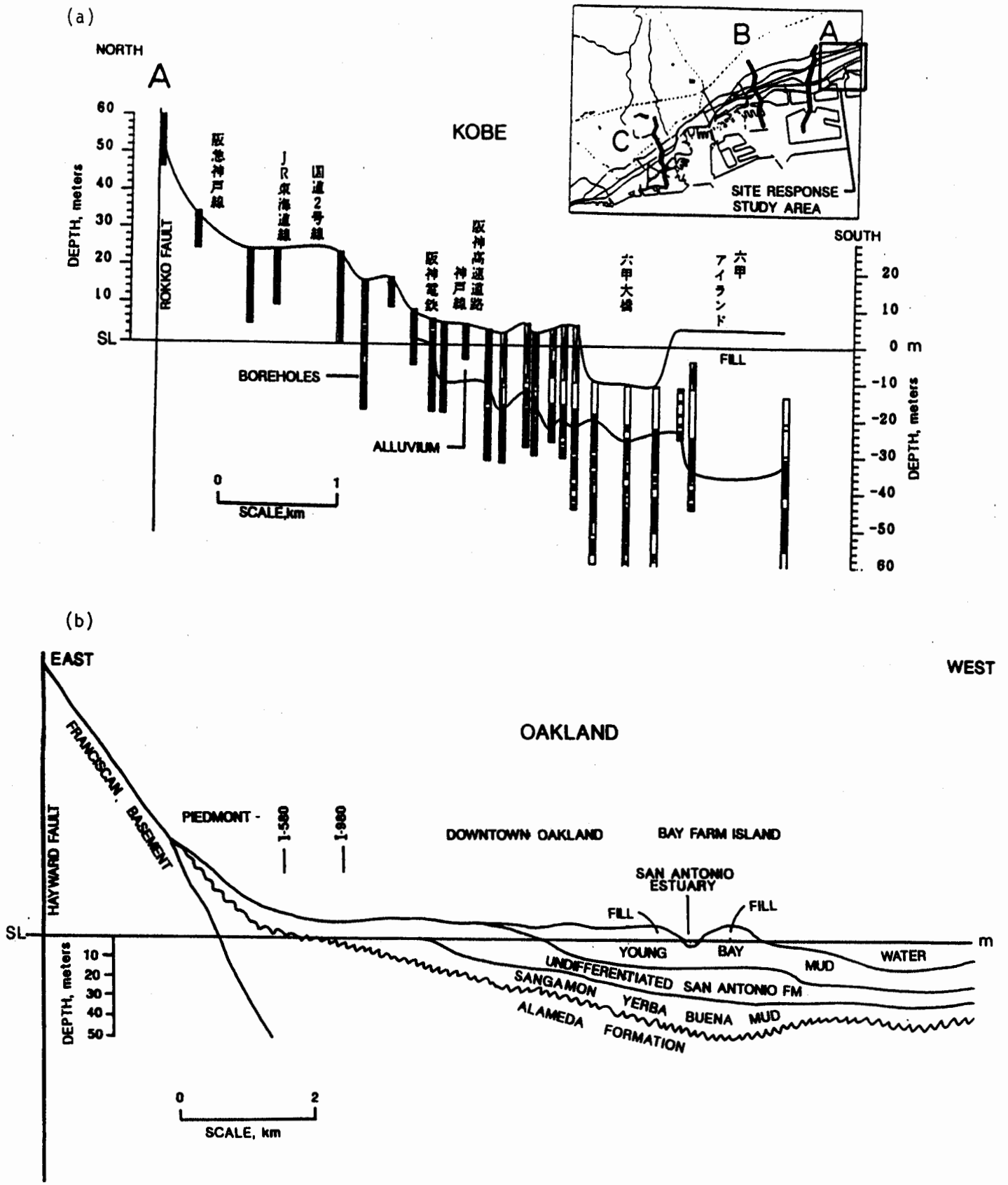

Figure 9. Profiles of shallow geological structure in Kobe (top) and Oakland (bottom; from Rogers and Figuers, 1991), with the Rokko and Hayward faults respectively on the left hand side of the profile. The inset in the Kobe profile locates the profile within the area shown in Figure 6, and also locates the site response study area shown in Figure 7. Both profiles have a vertical exaggeration of 30.

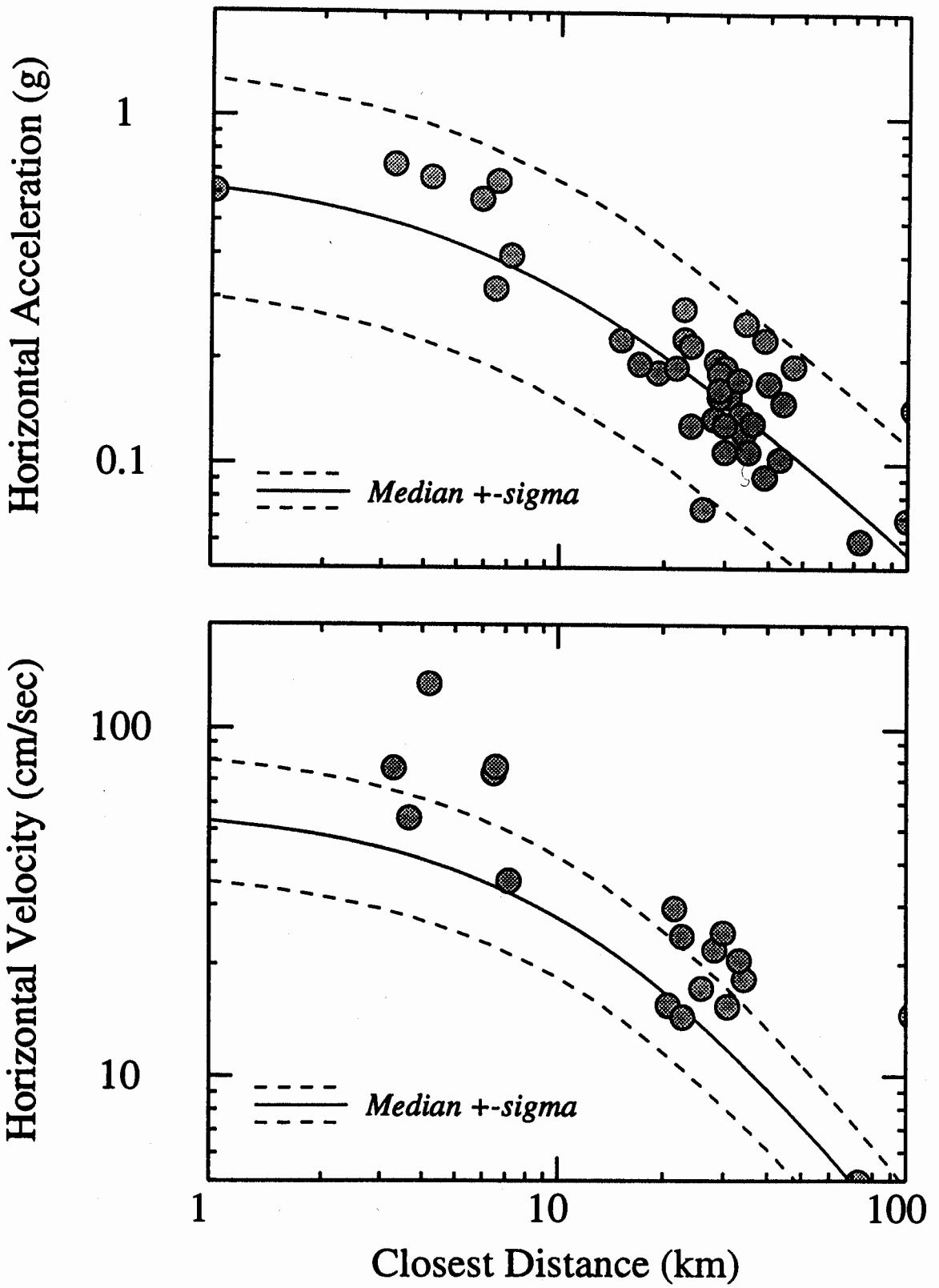

Figure 10. Attenuation of recorded peak acceleration and peak velocity at soil sites from the Kobe earthquake, compared with empirical relations for strike-slip earthquakes recorded on soil based mainly on California data (Abrahamson, 1995 for pga; Campbell, 1990 for pgv).